Optical Materials 90 (2019) 238–243

Contents lists available at ScienceDirect

Optical Materials

journal homepage: www.elsevier.com/locate/optmat

VUV excited luminescence and thermoluminescence investigation on Er^{3+}- or Pr^{3+}-doped BaY_2F_8 single crystals

Adriano B. Andrade[a,*], Giordano F. da C. Bispo[a], Zélia S. Macedo[a], Sonia L. Baldochi[b], Eduardo G. Yukihara[c,d], Mário E.G. Valerio[a]

[a] Physics Department, Federal University of Sergipe, São Cristovão, SE, 49100-000, Brazil
[b] Center for Lasers and Applications, IPEN/CNEN-SP, P.O. Box 11049, São Paulo, SP, 05422-970, Brazil
[c] Physics Department, Oklahoma State University, Stillwater, OK, 74078, USA
[d] Department of Radiation Safety and Security, Paul Scherrer Institute (PSI), Villigen PSI, Switzerland

ARTICLE INFO

Keywords:
BaY_2F_8
Luminescence
VUV spectroscopy
Thermoluminescence

ABSTRACT

Photoluminescence (PL), thermoluminescence (TL) emission spectra and TL glow curves of barium yttrium fluoride (BaY_2F_8 – BaYF), undoped and doped with erbium (Er^{3+}) or praseodymium (Pr^{3+}) were measured to investigate the fundamental absorption (band gap – E_g), the nature of the trapping centers, as well as the electronic transitions of Ln^{3+} in BaYF host. The band gap energy E_g of BaY_2F_8 was determined by vacuum ultraviolet (VUV) excitation measurements to be around 11.2 eV. Additionally, the electronic transition from excited states of Ln^{3+} ions and the exciton state were also identified. TL emission spectra showed that the TL emission of doped samples is related to the Ln^{3+} ion, indicating that the related host trapping centers are not affected by the new trapping centers originated due the dopant ions. Trap depths were calculated by fitting the glow curves using a first order kinetics model. Host-related trapping centers were attributed to intrinsic defects such as V_k and F centers and the new TL peaks observed for Er— and Pr-doped samples was associated to the electrons trapping centers. These results lead us to propose a simple model to explain the origin of the TL emission in BaYF.

1. Introduction

Barium Yttrium Fluoride (BaY_2F_8) is a well-known fast scintillator due to its cross-luminescence (CL) emission under exposure to ionizing radiation [1]. In the last years, BaY_2F_8 have been cited as a promising material for luminescence applications when doped with lanthanides ions: fast vacuum ultraviolet (VUV) scintillation when doped with Er^{3+} and Nd^{3+} or Tm^{3+} and Nd^{3+} [2,3], fast scintillating [4] when doped with Ce^{3+}, and also as a laser host when doped with Tm^{3+} [5] and Yb^{3+} [6]. Optical absorption results have shown that the scintillation of BaY_2F_8 is partly absorbed by centers created by the electrons and holes trapped at charge trapping centers related to host defects [7], decreasing the energy transfer efficiency from the host to the luminescent center [2].

Charge trapping centers have also been associated with the thermoluminescent (TL) signal in BaY_2F_8 [8]. The most probable intrinsic host defects in BaY_2F_8 has been attributed to the BaF_2 pseudo-Schottky [9], formed by two fluorine vacancies and one barium vacancy. The negative ion vacancy in alkaline halides form a F^+ center that can acts as an electrons trap, forming a defect like *F* center (an electron at a negative ion vacancy) [10]. On the other hand, it is known that the cation vacancy in alkaline halides works as a hole trapping center, forming a V_F center (like a V_K center adjacent to a cation vacancy), which is an antimorph of the F center [10,11].

The scintillating mechanism of Ln^{3+}-doped BaY_2F_8 be associated with the energy transfer from the host to the Ln^{3+} ions. However, the thermoluminescent mechanism emission is not yet completely understood. Kowalski et al. [12] showed for Nd^{3+}- and Ce^{3+}-doped BaY_2F_8 that their luminescent mechanism can be based on two possibilities; the first takes into account the self-trapped excitons to Ce^{3+}/Nd^{3+} radiative energy transfer, and the second and most probable assumes the capture of charge carries by Ce^{3+}/Nd^{3+}. In fact, lanthanide ions can work as charge trapping centers in wide bandgap materials [13], but the nature of the trapping center depends on the energy levels location within the band gap of the lanthanide ions [14].

In this work we proposed a simple model, based on our photoluminescence and TL results, to explain the origin of the charge trapping centers and TL signal of the BaY_2F_8 and the influence of the Er^{3+}

* Corresponding author.
E-mail address: abandrade1@gmail.com (A.B. Andrade).

https://doi.org/10.1016/j.optmat.2019.02.044
Received 30 November 2018; Received in revised form 5 February 2019; Accepted 24 February 2019
Available online 12 March 2019

and Pr^{3+} dopants in the TL emission. VUV measurement of our samples allowed us to estimate the BaY_2F_8 band gap energy (E_g). TL results showed that the host trapping centers are not affected by the presence of doping ion. On the other hand, the dopants added new trapping centers associated with TL peaks on the low temperature side of the host TL peak, as expected for Er and Pr working as electron traps. TL glow curves were fitted using GlowFit [15] computer program to estimate the trapping center depths.

2. Methodology

Undoped, Er^{3+}- or Pr^{3+}-doped BaY_2F_8 single crystals were grown by the zone melting method under HF atmosphere, from BaF_2 and YF_3 (and PrF_3) powders (previously prepared by standard fluorination method from their commercial carbonate and oxides, respectively) [16]. The raw materials were weighed and mixed in non-stoichiometric composition, according to the BaF_2-YF_3 phase diagram [17], with addition of LnF_3 (Ln = Er or Pr) for doped samples with 2.0 mol % concentration. The crystal growth procedure is described in more detail by Cruz [18]. Thermal analysis results indicated that BaY_2F_8 may actually be incongruent [17,18].

X-ray diffraction (XRD) in single crystalline powder samples was used to identify the crystalline phase. The measurements were carried out in a conventional Rigaku RINT 2000/PC diffractometer using Cu K alpha radiation, operating at 40 kV/40 mA, in the 2 theta range from 20° to 70°, using steps of 0.02°. The crystalline phase was confirmed by comparison with the standard patterns deposited in the Inorganic Crystal Structure Database (ICSD).

Photoluminescence excitation and emission measurements in the vacuum ultraviolet to visible range were measured at the Brazilian Synchrotron Light Laboratory (LNLS), using the facilities of the Toroidal Grating Monochromator (TGM) beamline [19]. The measurement details are described in previous works [20–23].

TL curve measurements were performed using a Risø TL/OSL-DA-15 reader (Risø National Laboratory, Denmark), equipped with a photomultiplier tube (PMT; model 9235QB, Electron Tubes Inc., Middlesex, UK) and a $^{90}Sr/^{90}Y$ beta irradiation source, delivering approximately 70 mGy/s in the sample position during exposure. The heating rate used was 5 K/s and high-purity N_2 was used in the heating chamber. A bandpass optical filter (Schott - BG39, 6.0 mm of total thickness, Schott AG) with transmission from ~340 nm to 610 nm, was used in front of the PMT. TL emission spectra were measured in a homemade TL reader replacing the PMT by an optical fiber connected to an Ocean Optics spectrometer (QE 65000 Pro, Ocean Optics Inc.). Each spectrum was recorded using an integration time of 1 s while the sample was heated at 5 K/s. The TL glow peak position measured by the spectrometer may show a difference of ± 15 K with respect to the TL curve measured using the Risø reader due to the lack of synchronization between the heating system and the optical fiber spectrometer acquisition, caused by the high heating rate used.

3. Results and discussions

Fig. 1 shows XRD powder patterns of the undoped and the Er^{3+}- or Pr^{3+} -doped BaY_2F_8 samples. All diffraction peaks for all the samples can be indexed to the BaY_2F_8 monoclinic belonging to the C12/m1(12) space group, consistent with the standard collection code 74359 obtained from the Inorganic Crystal Structure Database (ICSD) [24].

Fig. 2 shown the emission and excitation luminescence in VUV and visible region for the undoped sample. Under VUV excitation, undoped BaY_2F_8 exhibits a weak broad emission band with a maximum around 4.2 eV. This emission is attributed to the self-trapped excitons (STE) emission, that is almost completely thermally quenched at room temperature, as shown by Kirikova et al. [25]. The BaY_2F_8 can also exhibits a core-valence luminescence (CVL), due the radiative recombination process of an electron from the 2p level of the F^-, located in the valence

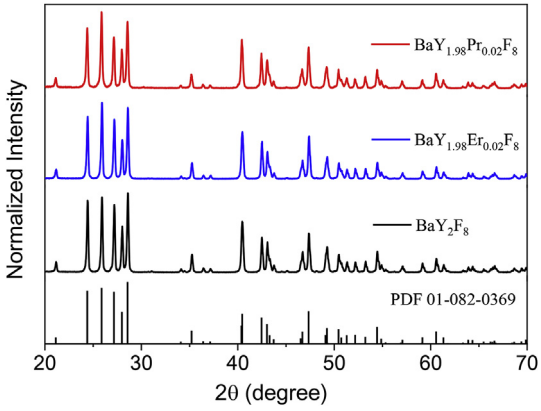

Fig. 1. X-ray diffraction measurements for the undoped and Er^{3+}- or Pr^{3+}-doped BaY_2F_8.

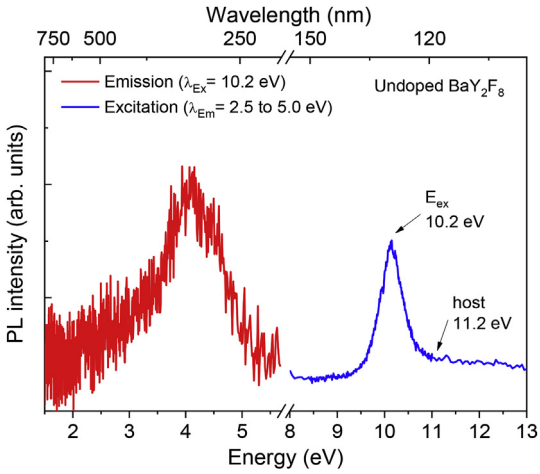

Fig. 2. Emission spectrum (red line) excited at 10.2 eV and excitation spectrum (blue line) monitoring the STE emission for the undoped BaY_2F_8. (For interpretation of the references to colour in this figure legend, the reader is referred to the Web version of this article.)

band with a hole in the 5p-core level of the Ba^{2+} [7]. However, it cannot be excited below 19.0 eV for BaY_2F_8 [1]. In general, this emission band is found for compounds containing Ba cations and F anions, such as $LiBaF_3$ [26], BaF_2 [1] and $BaLu_2F_8$ [7], being responsible for a well know fast emission. The excitation spectrum, recorded monitoring the emission in a range from 2.5 eV to approximately 5.0 eV, shows a broad excitation band centered at 10.2 eV. This band is similar to the one reported in Ref. [1], and is due to the excitonic absorption due the STE creation (E_{ex}) [25]. Therefore, it cannot be associated to the band gap energy (host) of BaY_2F_8. For this reason, we have used a relation proposed by Dorenbos in Ref. [27], which states that, for wide band gap materials, the exciton binding energy can be estimated by the expression $E_g = E_{ex} + (0.008 \times (E_{ex})^2)$. With this we found a reasonable value of 11.2 eV for the band gap energy of the BaY_2F_8, which is similar to the value reported by Becker et al. [28]. Furthermore, studies performed by Rubloff showed that the E_g can be estimated at about 1.0 eV above the exciton binding energy in fluoride materials [29].

Fig. 3 shows the excitation and emission spectra of the Er^{3+}-doped BaY_2F_8. The emission spectrum displays a series of narrow lines, which can be ascribed to the well-known intraconfigurational 4f-4f transitions of Er^{3+}. Also in Fig. 3, the excitation spectrum presents narrow bands associated to the 4f-5d transitions of Er^{3+}. The first high spin [HS] 5d-level and first low spin [LS] 5d-level were identified at 7.5 and 7.95 eV, respectively. The band centered at 10.2 eV, as discussed for the undoped BaY_2F_8, is associated to the STE creation (E_{ex}) [25]. A much less

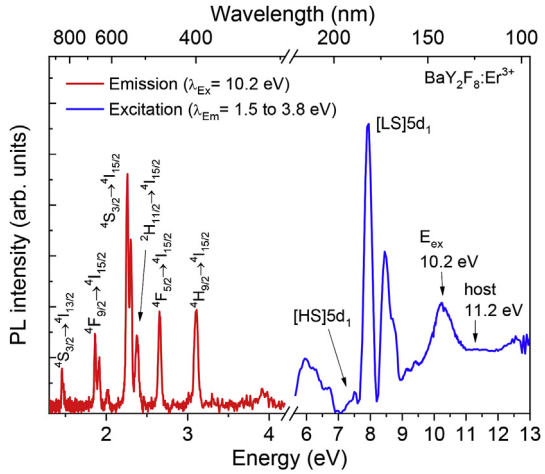

Fig. 3. Emission spectrum (red line) excited at 10.2 eV and excitation spectrum (blue line) monitoring the emission from Er^{3+} in a range of 1.5–3.8 eV. (For interpretation of the references to colour in this figure legend, the reader is referred to the Web version of this article.)

intense band located at around 11.2 eV is associated to the band gap energy. In fact, a low intensity band is expected in the excitation spectrum of Ln^{3+}-doped BaY_2F_8 due the low energy transfer efficiency from the host to the luminescent center [2,28].

Fig. 4 also shows the excitation and emission spectra, but for the Pr^{3+}-doped BaY_2F_8. In the emission spectrum it is possible to identify the interconfigurational $4f^15d^1 \rightarrow 4f^2$ transitions of the Pr^{3+} ions, exhibiting a characteristic broadband at the ultraviolet region in the range from 4.5 to 5.7 eV (~220–275 nm). In the range from 1.6 to ~2.8 eV the emission spectrum displays a series of narrow lines, which are ascribed to the intraconfigurational 4f-4f transitions of Pr^{3+}. The excitation spectrum in Fig. 4 is composed of $5d_1$, $5d_2$, $5d_4$ and $5d_5$ of Pr^{3+} excitation bands at 5.7, 6.6, 7.5 and 7.8 eV. The identification of the 5d levels of Pr^{3+} was done taking into account the well-established relation, which states that the energy of the $5d^1$ excitation band of Pr^{3+} can be predicted from the corresponding $5d^1$ excitation band observed for Ce^{3+} by simply adding (1.51 ± 0.09) eV energy [30]. Fabeni et al. [4], showed that the main 4f-5d transition of Ce^{3+}-doped BaY_2F_8 is located at 4.1 eV. So, using this relation we can find a value of ~5.7 eV for the $5d^1$ level of Pr^{3+}, which provides a good match with the value found in the excitation spectrum measured in the present work. Also in Fig. 4,

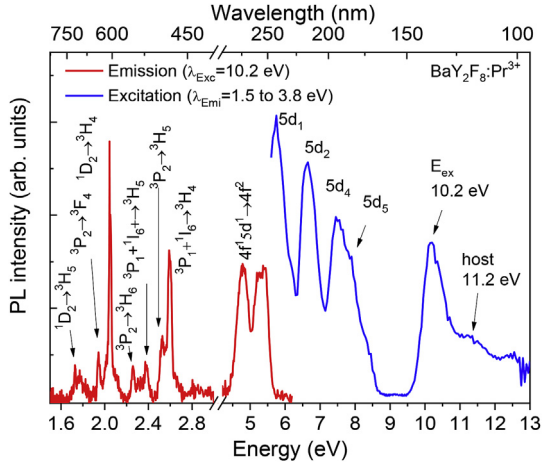

Fig. 4. Emission spectrum (red line) excited at 10.2 eV and excitation spectrum (blue line) monitoring the emission from Pr^{3+} in a range of 1.5–3.8 eV. (For interpretation of the references to colour in this figure legend, the reader is referred to the Web version of this article.)

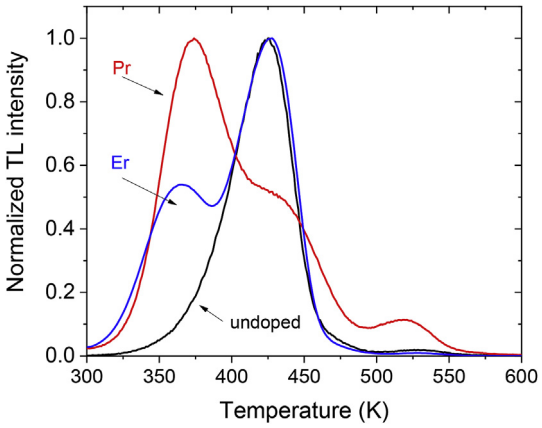

Fig. 5. Normalized TL curves of undoped, Er^{3+}- and Pr^{3+}-doped BaY_2F_8. All TL curves were recorded after exposure to the 20 Gy of beta radiation. The heating rate used was 5 Ks^{-1} and a visible transmitter filter Schott BG39 6 mm was used in front to PMT.

the bands centered at 10.2 and 11.2 eV, as discussed before, are ascribed to the STE creation and band gap energy, respectively.

Using the well-known redshift model, described by Dorenbos [30,31], we can predict the energy of the $5d_1$ levels for all Ln^{3+} ions if, for example, the experimental energy of 5d levels for Ce^{3+} is known. Thus, the predicted values obtained by the model for Er^{3+} and Pr^{3+} were 5.7 and 7.8 eV, while the values obtained from the excitation spectra (see Figs. 3 and 4) for Er^{3+} and Pr^{3+} were 5.7 and 7.5 eV, respectively, which represents a good agreement.

Fig. 5 shows the normalized TL curves for undoped and for Er^{3+}- and Pr^{3+}-doped BaY_2F_8. The TL curves were recorded after beta irradiation with a dose of 20 Gy. For the undoped sample, the TL curve consists of a characteristic non-symmetric first-order isolated TL peak, centered at 425 K, and a very weak TL peak at 530 K Er^{3+}-doped BaY_2F_8 also shows the same TL peaks related to the host at 425 and 530 K, as well as an additional TL peak located at a lower temperature (360 K). Pr^{3+}-doped BaY_2F_8 also shows at least one additional TL glow peak located at a lower temperature (365 K).

The origin of the TL emission of the undoped BaY_2F_8 is not yet fully known and the results in the literature up to now suggest that its TL emission is due trapping centers related to an intrinsic defect. As discussed by Amaral et al. [9], the most probable intrinsic defect in BaY_2F_8 host is BaF_2 pseudo-Schottky. In other words, this intrinsic defect is formed by one barium vacancy V'_{Ba} and two fluorine vacancies 2 $V^{\bullet}_{F}$, that can acts as holes and electrons trapping centers respectively, working as V_F and F centers. Besides this, it is well-known that the BaY_2F_8 STE emission of the BaY_2F_8 quenches increasing with temperature. However, the STE levels can still play a role in such energy transfer [2]. Thus, probably this can be the origin of the trapping centers responsible for the undoped BaY_2F_8 TL emission [8,32].

There are two possibilities for the new TL peaks observed for the Er^{3+}/Pr^{3+}-doped BaYF. Part of the excited charge carriers, electrons and holes, can be trapped either by host defects or lanthanide impurity levels. In fact, the lanthanides can trap electrons ($Ln^{3+} + e^- \rightarrow Ln^{2+}$) when their divalent 4f ground state is located few eV below the CB [13,14]. Free holes can be stabilized by interaction with two adjacent anions, creating a V_k-center, forming a self-trapped hole (STH). Furthermore, the energy of V_k-centers does not vary much for different fluoride host lattices, being the difference between the valence band and V_k-center of few eV [13]. Thus, it is not expected that the host TL peak would be affected by the presence of lanthanide ions. Thus, the presence of lanthanide ions would be responsible for existence of others related TL peaks.

On the other hand, the holes can also be trapped by trivalent 4f ground states ($Ln^{3+} + h^+ \rightarrow Ln^{4+}$) if they are located above intrinsic

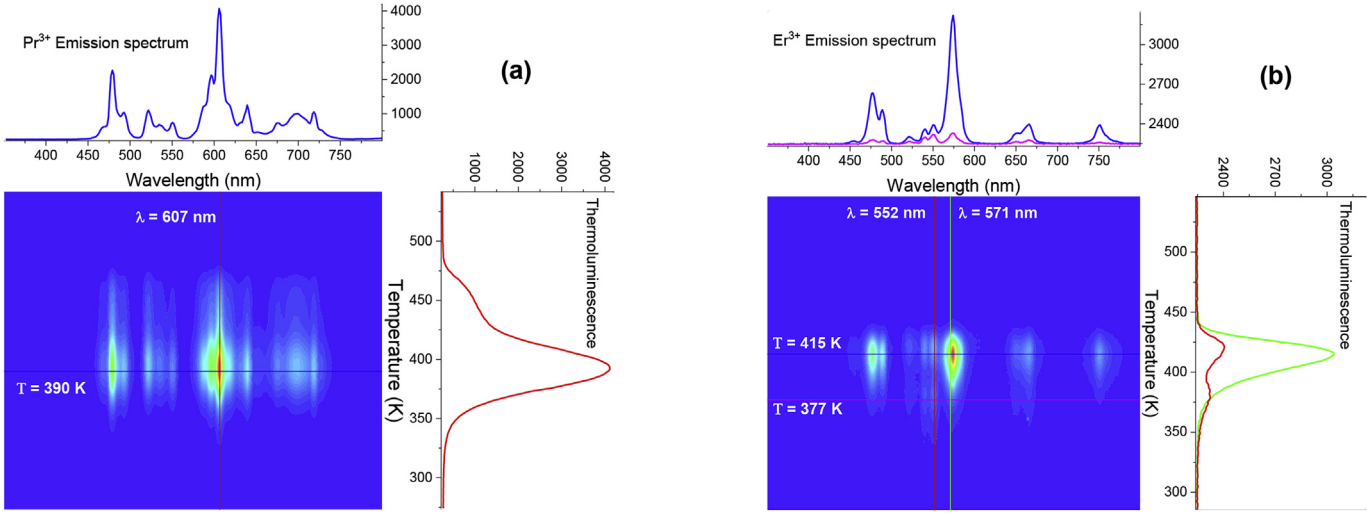

Fig. 6. TL emission spectrum of BaYF:Pr (a) and BaYF:Er (b). The samples were heated up to 673 K using a heating rate of 5 Ks^{-1} before irradiation to give a zero dose reference, followed of an irradiation for 300 s using an X-ray source delivering ~1.41 mGy/s at the sample position.

hole trapping center, relative to the VB [13]. Thus, the electron being released from an electron trapping center (intrinsic defect or divalent Ln state) recombine with a hole trapped at a trivalent Ln state or a self-trapped hole, or the Ln-trapped hole being released and recombine with a divalent Ln state, will result in an excited state of Ln^{3+}. Both processes will lead to a Ln^{3+} characteristic TL emission spectrum [13,14], as observed in Fig. 6(a) and (b).

Fig. 6(a) and (b) shows the TL emission spectrum of the Pr^{3+} and Er^{3+}-doped BaY_2F_8 samples, respectively. The emission spectrum for the undoped sample (not shown) was not detected in the range of the spectrometer (spectral response from 350 to 980 nm) or the emission was very weak to be detected by the spectrometer. Fig. 6(a) shows the contour plot with a main emission TL peak centered at 390 K. This TL emission is associated with Pr^{3+} emission, as observed in the emission spectrum on the top of Fig. 6(a). In Fig. 6(b) the contour graph shows that the TL emission for Er^{3+}-doped BaY_2F_8 is also composed by the characteristic emission from the dopant. Fig. 6(b) also shows that the TL curve (see TL curve on the right side of Fig. 6(b)) can display one or two TL peaks by monitoring different Er^{3+} emissions. Ln^{3+} TL emission spectrum was also reported for Ce^{3+}-doped BaY_2F_8 [33].

The presence of intrinsic electron and hole trapping centers can explain both intrinsic TL emission for undoped BaY_2F_8 and also the characteristic Ln^{3+} TL emission. However, which are the specific defect that is responsible for each peak is yet an open question. For example, if the process is governed by electron released, one should consider a Ln-trapped hole giving an excited 4f state of Ln^{3+}: $Ln^{4+} + e^{-} \rightarrow (Ln^{3+*})$. If the process is governed by hole released, one should consider a Ln-trapped electron giving an excited 4f state of Ln^{3+}: $Ln^{2+} + h^{+} \rightarrow (Ln^{3+*})$. In principle, both processes are equally possible and the mechanism that will dominate depend on the position of the 4f state of the lanthanide ion and the position of the host intrinsic defects. Additionally, the presence of shallow traps that may release trapped charges by thermal excitation at room temperature will lead to radiative recombination at Pr^{3+}/Er^{3+} and this is in line with the phosphorescent emission observed in a previous work for Pr^{3+}-doped BaY_2F_8 [32].

All above assumptions assume the existence of trapping centers associated to the host defects, and also additional trapping centers due to the presence of the Er^{3+} or Pr^{3+} levels. As observed in Fig. 5, the additional TL peaks for Er^{3+}/Pr^{3+}-doped samples are located at lower temperature range than the TL peaks related to the host. This indicates that Er^{3+}/Pr^{3+}-related TL peaks are due to shallower trapping centers. Thus, based on the above discussion, the activation energy of the TL peaks of all samples was investigated.

The trap depths E of the TL peaks were estimated assuming first-order kinetics. The choice of first-order kinetics is justified by TL measurements at various doses (not shown here), which revealed that the TL peak positions do not change with increasing doses of ionizing radiation. The fitted TL curves are shown in Fig. 7(a)-(c), and the obtained trapping parameters are listed in Table 1.

As discussed before and showed by the TL curve fitting, all of the samples showed the main TL peak related to the host with E ~ (0.74 ± 0.01) eV. For Er-doped BaY_2F_8, they show an additional TL peak at 362 K with E ~0.55 eV is presented, and for Pr-doped BaY_2F_8 they show two additional TL peaks at 370 and 395 K with E ~0.64 eV and E ~0.65 eV, respectively, were detected. These results showed that, regardless the Er^{3+} or Pr^{3+} dopant ion, the position and activation energy of the intrinsic TL peaks are virtually the same (see Table 1). Thus, based on the existence of holes and electrons traps related to the intrinsic defect on the host and also in the electron and hole storage capacity of the lanthanide states [14], it is possible to propose a model to explain the TL mechanism of the undoped and Er^{3+}/Pr^{3+}-doped BaY_2F_8.

For undoped BaY_2F_8, in principle, the TL mechanism can be governed by electron or hole release. Furthermore, as observed in Table 1, the position and activation energies of the host related TL peaks are not (or almost not affected) by the presence of new trapping centers created by the dopants. However, for Er/Pr-doped samples we can consider a mechanism governed by electron release from the divalent lanthanide 4f ground state and/or from an intrinsic electron trapping center. The electron will recombine with a Ln-trapped hole resulting in an excited 4f of the Ln^{3+}. This mechanism is corroborated by the additional TL peaks at lower temperature for Er/Pr-doped BaY_2F_8 since the activation energies found for TL peaks related to the Er/Pr doping ions are according to expected for Er^{2+} and Pr^{2+} states. Typically, the Ln^{2+} (as Er^{2+} and Pr^{2+}) state are located close and just below of the CB in wide gap materials, as showed for different fluoride hosts by the energy levels scheme developed by Dorenbos [34]. Thus, it is reasonable to consider that the host electron trapping center is located below that Ln^{2+} states of the Er and Pr (relative to CB). However, if a TL mechanism now governed by hole-release from self-trapped holes or from holes trapped by Ln dopants is considered, one should expect that the TL peak would be at a much higher temperature since the trap depth for holes trapped in the 4*f* state of lanthanide ions are located well above the valence band, acting as deep trapping centers [14]. Since higher temperature TL peaks were not detected, this mechanism has to be ruled out, only the mechanism due to electron-release is possible. Fig. 8 illustrates the TL scheme summarizing the TL mechanism discussion via

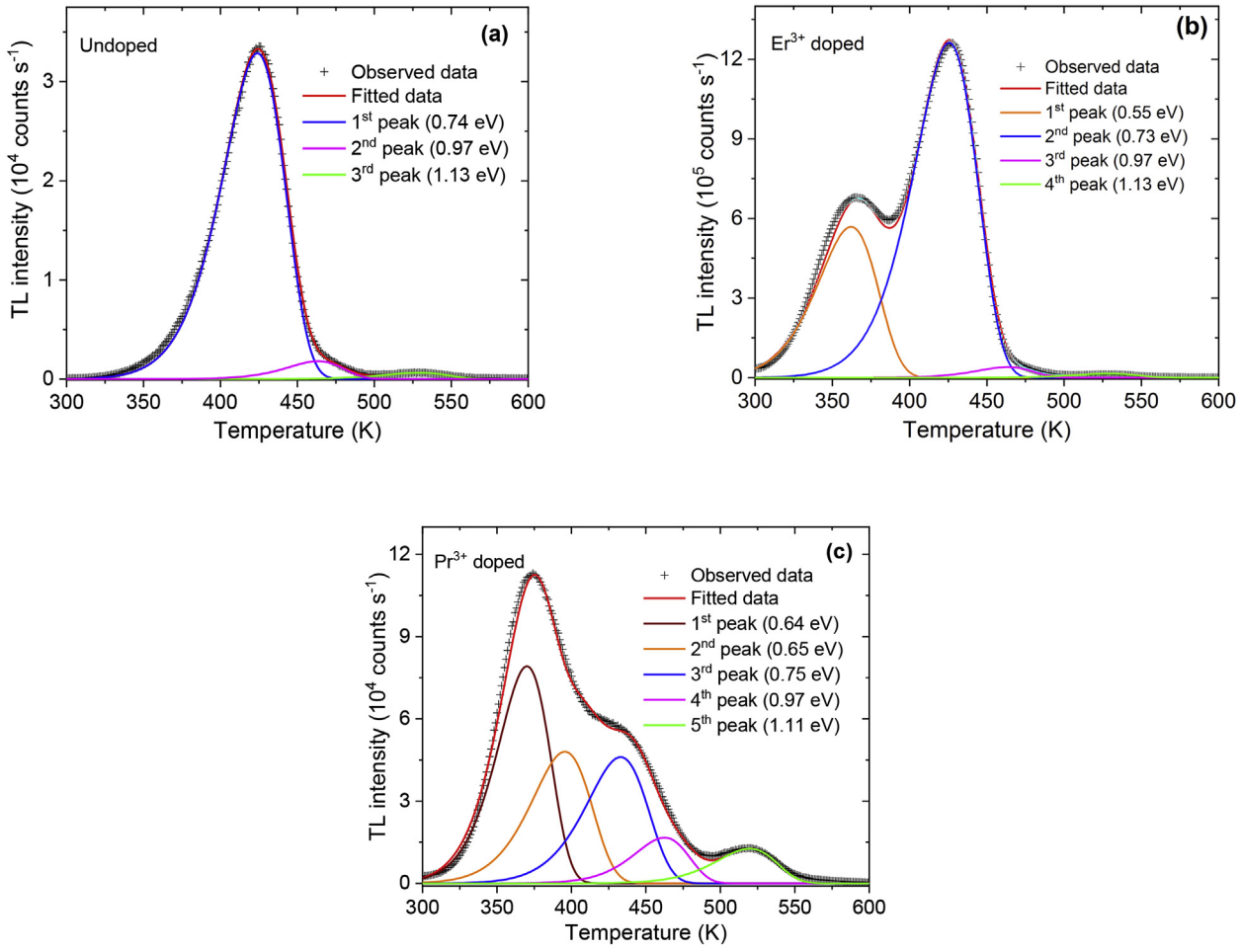

Fig. 7. TL curve-fitted data using the first-order kinetics model. (a) Undoped BaYF, (b) Er-doped BaY_2F_8 and (c) Pr-doped BaY_2F_8. All TL curves were recorded after exposure to the 20 Gy of beta radiation. The heating rate used was 5 Ks^{-1} and a visible transmitter filter Schott BG39 6 mm was used in front to PMT.

Table 1
TL parameters obtained by curve fitting for the undoped and doped samples.

	Sample		
	BaYF:Pr	BaYF:Er	BaYF
Tm (K)	370	–	–
Act. E. (eV)	0.64	–	–
Tm (K)	395	362	–
Act. E. (eV)	0.65	0.55	–
Tm (K)	432	425	424
Act. E. (eV)	0.75	0.73	0.74
Tm (K)	462	463	463
Act. E. (eV)	0.97	0.97	0.97
Tm (K)	528	528	528
Act. E. (eV)	1.11	1.13	1.13

electron releasing.

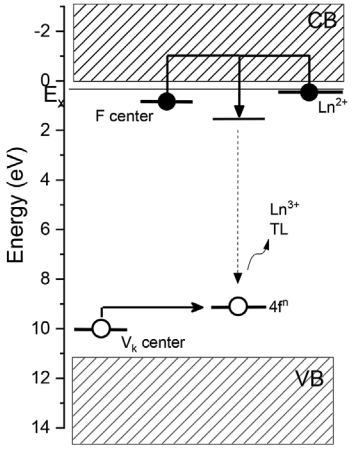

Fig. 8. Simple model to explain the Ln^{3+} emission at TL curve for Er— or Pr-doped BaYF.

4. Conclusions

The results reported in this work support the discussion regarding the luminescent mechanism of the undoped and Er^{3+}- or Pr^{3+}-doped BaYF single crystals. Photoluminescence excitation results measured in VUV range showed that the energy needed to create the exciton is about 10.2 eV and the fundamental absorption (band gap energy) is located at 11.2 eV. These results indicated that the host to luminescent center energy transfer process in BaYF is poor efficient for excitation energy ≥ to E_g. The emission spectra for undoped sample showed that the intrinsic luminescence at room temperature is rather weak. On the other hand, the luminescence from Er and Pr doped samples were quite efficient.

Thermoluminescence results showed the existence of TL peaks related to the intrinsic host defects due the presence of F and V_k-centers. Additional TL peaks were observed for Er^{3+} and Pr^{3+}-doped BaYF and showed a TL emission spectra characteristic of the intraconfigurational 4f-4f transition of the dopant. All TL peaks were assigned to first order

kinetics and depths of trapping centers, calculated by using the TL peak fit method, suggested that the additional TL peak, for doped samples are due the shallow electrons traps. Besides this, TL peaks from the host are not affected by the dopant related traps. Thus, we can conclude that the host related defects are not affected by the shallow electron traps created by the presence of the Er and Pr dopants.

Acknowledgments

This research was partially supported by CAPES and CNPq, Brazilian funding agencies. The authors thanks to the Brazilian Synchrotron Light Laboratory (LNLS) under proposal ID 20180002. Adriano B. Andrade thanks FAPITEC/SE (grants: 12737.410.23852.15012018).

References

[1] Y.M. Aleksandrov, I.L. Kuusmann, V.N. Makhov, S.B. Mirov, T. V Uvarova, M.N. Yakimenko, Intrinsic and impurity cross-luminescence in three-component barium-containing compounds, Nucl. Instrum. Methods Phys. Res. Sect. A Accel. Spectrom. Detect. Assoc. Equip. 308 (1991) 208–210 https://doi.org/10.1016/0168-9002(91)90628-4.

[2] J. Pejchal, M. Nikl, F. Moretti, A. Vedda, K. Fukuda, N. Kawaguchi, T. Yanagida, Y. Yokota, A. Yoshikawa, Luminescence mechanism and energy transfer in doubly-doped BaY 2 F 8 :Tm,Nd VUV scintillator, IOP Conf. Ser. Mater. Sci. Eng. 15 (2010) 12018 http://stacks.iop.org/1757-899X/15/i=1/a=012018.

[3] J. Pejchal, M. Nikl, K. Fukuda, N. Kawaguchi, T. Yanagida, Y. Yokota, A. Yoshikawa, V. Babin, Doubly doped BaY2F8:Er,Nd VUV scintillator, Radiat. Meas. 45 (2010) 265–267 https://doi.org/10.1016/j.radmeas.2009.10.017.

[4] P. Fabeni, D. Di Martino, M. Nikl, G.P. Pazzi, E. Sani, A. Toncelli, M. Tonelli, A. Vedda, Optical properties of BaY2F8:Ce3+, Phys. Status Solidi 2 (2005) 244–247, https://doi.org/10.1002/pssc.200460156.

[5] G. Galzerano, F. Cornacchia, D. Parisi, A. Toncelli, M. Tonelli, P. Laporta, Widely tunable 1.94-?mTm:BaY2F8 laser, Opt. Lett. 30 (2005) 854–856, https://doi.org/10.1364/OL.30.000854.

[6] S. Bigotta, D. Parisi, L. Bonelli, A. Toncelli, M. Tonelli, A. Di Lieto, Spectroscopic and laser cooling results on Yb3+-doped BaY2F8 single crystal, J. Appl. Phys. 100 (2006) 13109, https://doi.org/10.1063/1.2211633.

[7] J.C. van 't Spijker, P. Dorenbos, C.W.E. van Eijk, J.E.M. Jacobs, H.W. den Hartog, N. Korolev, Luminescence and scintillation properties of BaY2F8:Ce3+, BaLu2F8 and BaLu2F8:Ce3+, J. Lumin. 85 (1999) 11–19 https://doi.org/10.1016/S0022-2313(99)00154-4.

[8] A.C.S. De Mello, A.B. Andrade, G.H.G. Nakamura, S.L. Baldochi, M.E.G. Valerio, Luminescence properties of Er3+ and Tm3+ doped BaY2F8, J. Lumin. 138 (2013) 19–24.

[9] J.B. Amaral, M.A. Couto dos Santos, M.E.G. Valerio, R.A. Jackson, Computer modelling of BaY2F8: defect structure, rare earth doping and optical behaviour, Appl. Phys. B 81 (2005) 841–846, https://doi.org/10.1007/s00340-005-1933-z.

[10] C.M. Sunta, Induction of Thermoluminescence, (2015), pp. 15–28, https://doi.org/10.1007/978-81-322-1940-8_2.

[11] V.I. Dubinko, A.A. Turkin, D.I. Vainshtein, H.W. den Hartog, Theory of the late stage of radiolysis of alkali halides, J. Nucl. Mater. 277 (2000) 184–198, https://doi.org/10.1016/S0022-3115(99)00207-X.

[12] Z. Kowalski, S.M. Kaczmarek, K. Brylew, W. Drozdowski, Radioluminescence as a function of temperature and low temperature thermoluminescence of BaY2F8:Ce and BaY2F8:Nd crystals, Opt. Mater. (Amst). 59 (2016) 145–149 https://doi.org/10.1016/j.optmat.2015.12.047.

[13] A.H. Krumpel, E. van der Kolk, D. Zeelenberg, A.J.J. Bos, K.W. Krämer, P. Dorenbos, Lanthanide 4f-level location in lanthanide doped and cerium-lanthanide codoped NaLaF4 by photo- and thermoluminescence, J. Appl. Phys. 104 (2008) 73505, https://doi.org/10.1063/1.2955776.

[14] A.J.J. Bos, P. Dorenbos, A. Bessière, B. Viana, Lanthanide energy levels in YPO4, Radiat. Meas. 43 (2008) 222–226 https://doi.org/10.1016/j.radmeas.2007.10.042.

[15] M. Puchalska, P. Bilski, GlowFit—a new tool for thermoluminescence glow-curve deconvolution, Radiat. Meas. 41 (2006) 659–664 https://doi.org/10.1016/j.radmeas.2006.03.008.

[16] S.L. Baldochi, I.M. Ranieri, A short review on fluoride laser crystals grown by czochralski method at IPEN, Acta Phys. Pol., A 124 (2013) 286, https://doi.org/10.12693/APhysPolA.124.286.

[17] G.H.G. Nakamura, S.L. Baldochi, V.L. Mazzocchi, C.B.R. Parente, M.E.G. Valério, D. Klimm, Problems in the thermal investigation of the BaF2-YF3 system, J. Therm. Anal. Calorim. 95 (2009) 43–48, https://doi.org/10.1007/s10973-008-9005-3.

[18] S.F. de A. Cruz, Ph.D. Thesis, Crescimento e caracterização de monocristais de BaY2F8:TR onde TR = Nd3+, Pr3+, Er3+, Tb3+, Dy3+ vol. 1, Univ. São Paulo, 2008, http://www.teses.usp.br/teses/disponiveis/85/85134/tde-13102011-103049/pt-br.php.

[19] R.L.C. Filho, A.F. Lago, M.G.P. Homem, S. Pilling, A.N. de Brito, Delivering high-purity vacuum ultraviolet photons at the Brazilian toroidal grating monochromator (TGM) beamline, J. Electron. Spectrosc. Relat. Phenom. 156–158 (2007) 168–171 https://doi.org/10.1016/j.elspec.2006.11.026.

[20] A.B. Andrade, M.E.G. Valerio, Structural and optical properties of the nanopowder of the Eu3+ doped LiLaP4O12 produced by sol gel route, Radiat. Meas. 71 (2014) 55–60.

[21] C. dos S. Bezerra, M.E.G. Valerio, Structural and optical study of CaF2 nanoparticles produced by a microwave-assisted hydrothermal method, Phys. B Condens. Matter 501 (2016) 106–112 https://doi.org/10.1016/j.physb.2016.08.025.

[22] G.F.C. Bispo, A.B. Andrade, C.D. S Bezerra, V.C. Teixeira, D. Galante, M.E.G. Valerio, Luminescence in undoped $CaYAl_3O_7$produced via the Pechini method, Phys. B Condens. Matter 507 (2017), https://doi.org/10.1016/j.physb.2016.12.002.

[23] A.B. Andrade, N.S. Ferreira, M.E.G. Valerio, Particle size effects on structural and optical properties of BaF2 nanoparticles, RSC Adv. 7 (2017) 26839–26848, https://doi.org/10.1039/C7RA01582H.

[24] L.H. Guilbert, J.Y. Gesland, A. Bulou, R. Retoux, Structure and Raman spectroscopy of czochralski-grown barium yttrium and barium ytterbium fluorides crystals, Mater. Res. Bull. 28 (1993) 923–930 https://doi.org/10.1016/0025-5408(93)90039-G.

[25] N.Y. Kirikova, V. Klimenko, V. Kozlov, V. Makhov, N. Khaidukov, T. Uvarova, Cross-luminescence of several complex fluorides excited by synchrotron radiation, Nucl. Instrum. Methods Phys. Res. Sect. A Accel. Spectrom. Detect. Assoc. Equip. 359 (1995) 351–353, https://doi.org/10.1016/0168-9002(94)01383-7.

[26] P.A. Rodnyi, M.A. Terekhin, E.N. Mel'chakov, Radiative core-valence transitions in barium-based fluorides, J. Lumin. 47 (1991) 281–284 https://doi.org/10.1016/0022-2313(91)90051-V.

[27] P. Dorenbos, Charge transfer bands in optical materials and related defect level location, Opt. Mater. (Amst). 69 (2017) 8–22 https://doi.org/10.1016/j.optmat.2017.03.061.

[28] J. Becker, J. Gesland, N.Y. Kirikova, J. Krupa, V. Makhov, M. Runne, M. Queffelec, T. Uvarova, G. Zimmerer, Fast VUV emission of rare earth ions (Nd3+, Er3+, Tm3+) in wide bandgap crystals, J. Alloy. Comp. 275–277 (1998) 205–208, https://doi.org/10.1016/S0925-8388(98)00304-1.

[29] G.W. Rubloff, Far-ultraviolet reflectance spectra and the electronic structure of ionic crystals, Phys. Rev. B 5 (1972) 662–684, https://doi.org/10.1103/PhysRevB.5.662.

[30] P. Dorenbos, Exchange and crystal field effects on the 4f n −1 5d levels of Tb 3+, J. Phys. Condens. Matter 15 (2003) 6249 http://stacks.iop.org/0953-8984/15/i=36/a=313.

[31] P. Dorenbos, The 4fn↔4fn−15d transitions of the trivalent lanthanides in halogenides and chalcogenides, J. Lumin. 91 (2000) 91–106 https://doi.org/10.1016/S0022-2313(00)00197-6.

[32] A.B. Andrade, A.C.S. de Mello, M.V. dos S. Rezende, S.L. Baldochi, M.E.G. Valerio, Optical properties of Pr-doped BaY2F8, J. Appl. Phys. 116 (2014) 053521, , https://doi.org/10.1063/1.4892111.

[33] A. Vedda, M. Martini, D.D.I. Martino, E. Sani, A. Toncelli, M. Tonelli, Thermally stimulated luminescence properties of BaY 2 F 8 :Ce crystals, Radiat. Eff. Defect Solid 157 (2002) 973–976, https://doi.org/10.1080/10420150215774.

[34] P. Dorenbos, Systematic behaviour in trivalent lanthanide charge transfer energies, J. Phys. Condens. Matter 15 (2003) 8417 http://stacks.iop.org/0953-8984/15/i=49/a=018.